sustainability

MDPI

Article

Slope Scaling Effect and Slope-Conversion-Atlas for Typical Water Erosion Regions in China

Xue Chen [1], Guokun Chen [1,2,*], Junxin Feng [1], Jingjing Zhao [1] and Yiwen Wang [1]

[1] Faculty of Land Resource Engineering, Kunming University of Science and Technology, Kunming 650093, China
[2] Key Laboratory of Plateau Remote Sensing, Yunnan Provincial Department of Education, Kunming 650093, China
* Correspondence: chengk@radi.ac.cn

Abstract: Slope has obvious scale-dependent characteristics and it changes with the change in DEM resolution, which brings uncertainty to the evaluation process of regional resource and environment. In this paper, one typical county in each of the six water erosion regions in China was selected as the sample area, respectively. Based on DEM data of ALOS DEM, ASTER GDEM and SRTM DEM with different spatial resolutions, slope characteristics, such as gradient, eigenvalue, frequency and cumulative frequency curves, were calculated by using the third-order inverse distance square weighted difference algorithm, to explore the ability of depicting terrain by these three DEM data. Based on the idea of geo-information map, the "surface-slope conversion atlas" under different resolutions was constructed to achieve the grading correction of slope extraction under low resolution. The results showed that: (1) with the resolution of DEM decreases, the slope information of each area tends to be more generalized and gradually concentrated. The slope frequency curve gradually changed from "tall and thin" to "short and fat", and the peak of the cumulative frequency curve moved to the low-slope area. Six sample areas showed different degrees of slope reduction. (2) In the process of slope grading correction, except for Maoxian, the proportion of low-resolution results converted to medium and low slope grades (0°–25°) is large. (3) The slope spectrum conversion method has a good correction effect on the errors generated by the slope extraction results of DEM_{90} and DEM_{30}, and the correction rates reached 80% and 90%, respectively. A slope conversion atlas can effectively improve the expression ability of low-resolution DEM data on topography, which can provide a basis for regional resource and environment evaluation, and territorial space optimization.

Keywords: scale effect; DEM; regional scale; slope-conversion-atlas; resolution; water erosion

Citation: Chen, X.; Chen, G.; Feng, J.; Zhao, J.; Wang, Y. Slope Scaling Effect and Slope-Conversion-Atlas for Typical Water Erosion Regions in China. *Sustainability* **2023**, *15*, 3789. https://doi.org/10.3390/su15043789

Academic Editor: Hariklia D. Skilodimou

Received: 28 December 2022
Revised: 29 January 2023
Accepted: 15 February 2023
Published: 19 February 2023

1. Introduction

Topographic factors are the critical input parameters in many earth surface processes such as soil erosion, which are very important for quantitatively monitoring and forecasting sustainability of resources and environment [1–4]. For water erosion assessment at large spatial scales, extraction of slope features is inseparable from DEM resolution [5,6], and the effect of slope scale issues on erosion is very significant. As the model is an abstract description of the surface process, the appropriate selection of DEM directly affects the accurate calculation of slope, and thus affects the final estimation of surface geographical phenomena, and all links in the process [7–12]. However, due to the limitations of data acquisition and quality, calculation time, data volume, research scope, and other factors, slope is generally extracted by DEM of medium-low resolution DEMs [13].

Scale effects, which refers to the change in object expression and analysis results caused by the change in scale, widely exist in various geographical phenomena and processes on the Earth's surface [14]. As a digital terrain model, DEM expresses the continuously changing surface morphology in a discrete way, which is inevitably constrained by scale.

Thus, the topographic parameters calculated based on DEM have obvious scale-dependent characteristics in resource environment evaluation [15–18]. Because the geographical space is infinitely complex, it is impossible for people to observe all the details of the real geographical world. Therefore, the description of the surface by geographic information is always approximate, and the degree of this approximation reflects the degree or scale of abstraction of geographical phenomena and processes. Therefore, scale is the basic and important feature of all geographic information, and the information expressed by different scales is very different. The scale problem has also been listed in the top ten priority areas of future research in geographic information science by USGS [19].

There are significant differences between hillside and river systems extracted by different DEMs, and slope values may be overestimated or underestimated in different areas [20,21]. A large number of studies have confirmed the scale effect of topographic factors [22–25], and the results show that, with the decrease in DEM resolution, the ground fluctuation cannot be well represented, which introduces uncertainty into the evaluation results of soil erosion at regional scale [12,26,27]. Related research shows that, by comparing the characteristics of topography at six different resolutions of DEM, the relationship between topography and DEM resolution does not always show a linear relationship [28]. The study of Quinn et al. shows that the terrain index based on coarse resolution DEM increases and the slope decreases [29].

The well-known soil erosion topographic factors (LS) was calculated using DEMs from five different data sources, and it was concluded that the accuracy of LS factor calculation decreases with decreasing resolution of topographic data sources [30]. A study of terrain representation and recognition capability based on different resolution DEMs and different algorithms shows that the terrain recognition capability of different algorithms also varies with the resolution [31]. Therefore, the analysis of slope attenuation introduced by low- and medium-resolution DEMs and the scaling transformation of slopes is essential. The accuracy of the converted results can be comparable to the higher resolution data to reflect actual topographic relief, which is particularly important to solve the contradiction between the relatively low resolution of available data for regional scale assessment, and the requirement of high resolution of surface geographical phenomena and processes.

In view of the demand for slope index and slope attenuation in large-scale research [32,33], relevant scholars have explored slope scaling based on landform surface slope spectrum characteristics [34] and fractal characteristics [35–37]. At present, the slope transformation methods of low-medium resolution mainly include slope mapping transformation [38–40], fractal transformation [35,41], and histogram matching transformation [22,42,43]. Among them, the methods based on slope spectrum and histogram matching transformation are intuitive and can visually express the variation of terrain attributes at different scales. The fractal transformation utilizes the self-similarity between local and whole fractal objects to perform slope conversion between different scales [44].

In terms of applications, some scholars analyzed the scale correlations at watershed scale [17], and DEM resolution sensitivity and effective parameters on runoff yield using the SWAT model [18], as well as watershed-based hydrologic simulation [45]. Tang et al. [39] took small watershed in a hilly area of the Loess Plateau as the research object, and found that the slope conversion map could effectively correct the statistical values of surface slope. Liu et al. [46] studied the Jiuyuangou watershed in Suide County, northern Shaanxi as the experimental sample area, and concluded that the slope conversion map could correctly estimate the accuracy of topographic factors such as the slope extracted by DEM. Liu Xinhua [47] pointed out that the slope conversion map is an effective method for scale conversion between different scales. Niu et al. [48] chose a regression statistical method based on the "surface slope conversion atlas" to obtain the quadratic fitting curve corresponding to each slope grade and considered this method as an effective way for improving the statistical accuracy of the slope. Guo et al. [35] used geomorphic fractal characteristics to transform, and proposed that the optimal range of slope transformation is 0.2 to 0.25 times of the original resolution slope. Meng T [41] combined fractal and

semi-variance functions to convert the slope units extracted by a low resolution of DEM to "real" terrain slope values. Yang et al. [22] applied the histogram matching principle to slope scaling for the first time, realizing the consistent expression of low-resolution data after conversion and high-resolution slopes. Shi [49] utilized the histogram matching principle to establish the slope transformation relationship between adjacent scales, so that the eigenvalues and spatial structures after slope transformation can better reflect the ground undulation. Panuska compared DEMs from 15 m to 90 m grid sizes, and found that the confluence area was larger when the separation rate was small [50]. Yang [51] established a downscaling model based on the histogram matching principle, and found that the downscaling model for slope length is not as effective as the downscaling model for slope degree.

However, the relevant studies mainly focus on a single area such as the Loess Plateau area on a micro-spatial scale or connected with physical models such as SWAT and WEPP, and the applicability and differences of the proposed slope transformation method for regional scale or larger areas are yet to be investigated.

In this paper, one county sensitive to severe erosion in each of the six national water erosion regions in China was selected as the study sample area. Based on three different resolutions of DEM data, the differences of topographic features extracted from different areas at different resolutions will be compared. Based on the previous transformation method, this paper attempts to rectify the extraction results of commonly used low resolution of DEM (90 m, 30 m) with reference to the 10 m resolution slope where the terrain is more finely carved, which allows the slope to reflect the topography more accurately after correction, so as to provide a basis for regional resource and environmental evaluation of complex terrain.

2. Materials and Methods

2.1. Study Area

According to the national regionalization scheme of soil and water conservation (Figure 1), as well as severe soil erosion counties demarcated by the Ministry of Water Resources of China [52], we selected one typical county in each of the six water erosion dominated regions as the study area. Specifically, (a) Dongfeng in the Northeast Black Soil Region (NBSR, low-hilly landforms); (b) Mengyin in the North Rocky Mountain Region (NRMR, characterized by low hills and relatively flat terrain); (c) Luochuan in the Northwest Loess Plateau Region (NLPR, loess beam-shaped hills and loess tableland, one of the most serious areas of soil erosion worldwide and the main source of sediment in the Yellow River); (d) Yudu in the South Red Soil Region (SRSR, mid-mountains, hills and basins); (e) Maoxian in the Southwest Purple Soil Region (SPSR, high mountains and intermountain valleys); (f) Yuanmou in the Southwest Karst Mountainous Region (SKMR, high mountain landforms, tectonic denudation mid-mountain hilly landforms, and fractured basin accumulation landforms) (Figure 2).

2.2. Data Source and Data Pre-Processing

Critical data in this study were obtained as follows: ALOS DEM, ASTER GDEM v2 and SRTM DEM with different spatial resolutions (12.5 m, 30 m and 90 m, respectively) are prepared to derive topographical parameters, hereinafter referred as $DEM_{12.5}$, DEM_{30} and DEM_{90}, respectively. All these data were converted and pre-processed (format conversion, DEM data stitching and projection transformation) before incorporated as input layers for further analysis.

In order to ensure the correspondence between the calculated results of DEM with different resolutions, ALOS DEM (12.5 m) was resampled to 10 m and marked as DEM_{10}. As can be seen in Figure 3, each DEM grid cell with a resolution of 30 m corresponds to 3×3 10 m resolution grids. Similarly, for each 90 m DEM grid cell, there are 9×9 10 m resolution grids corresponding to it.

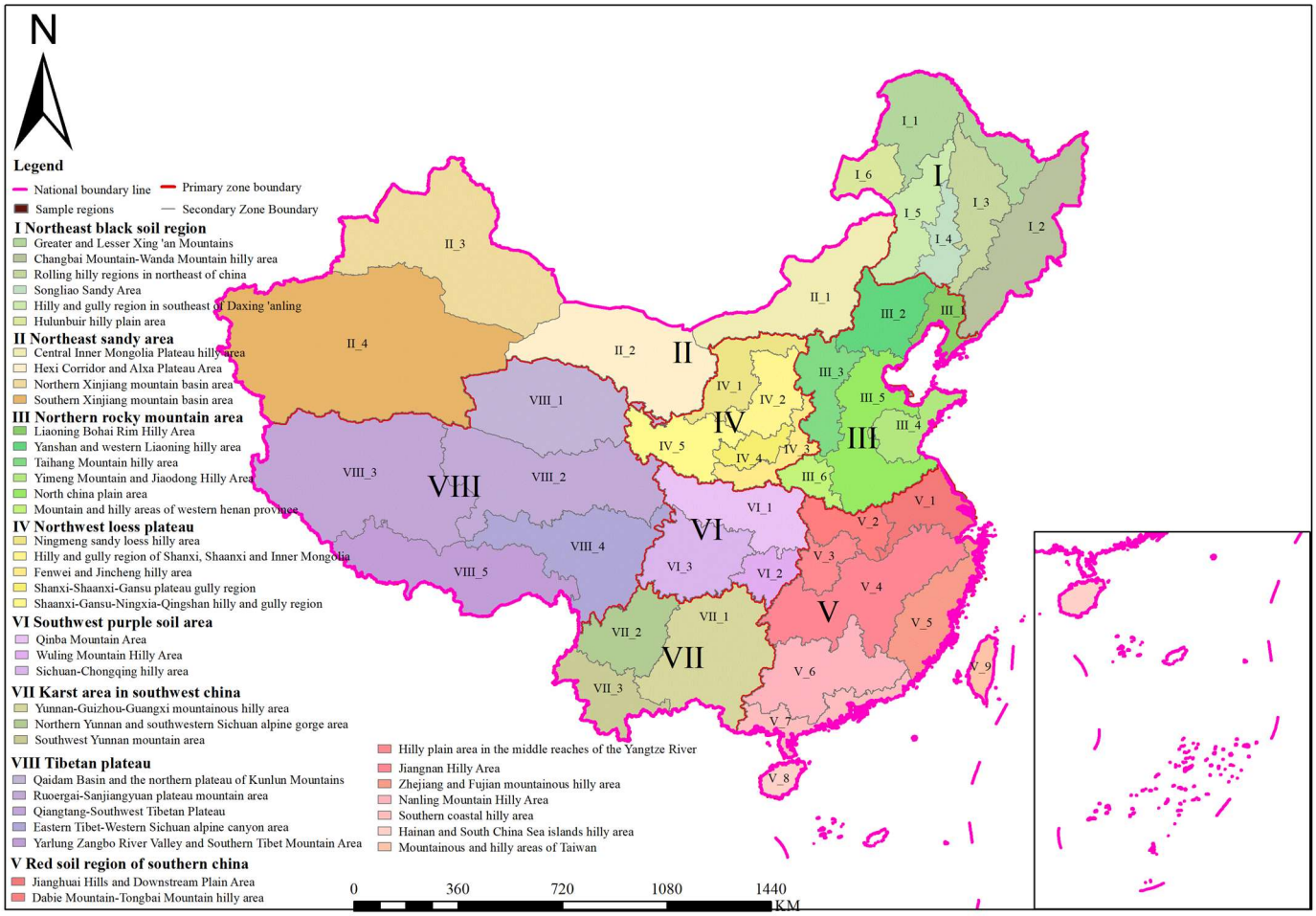

Figure 1. Soil and water conservation regionalization map of China: Except for II (dominated by wind erosion) and VIII (dominated by frozen erosion), the rest are typical water erosion regions.

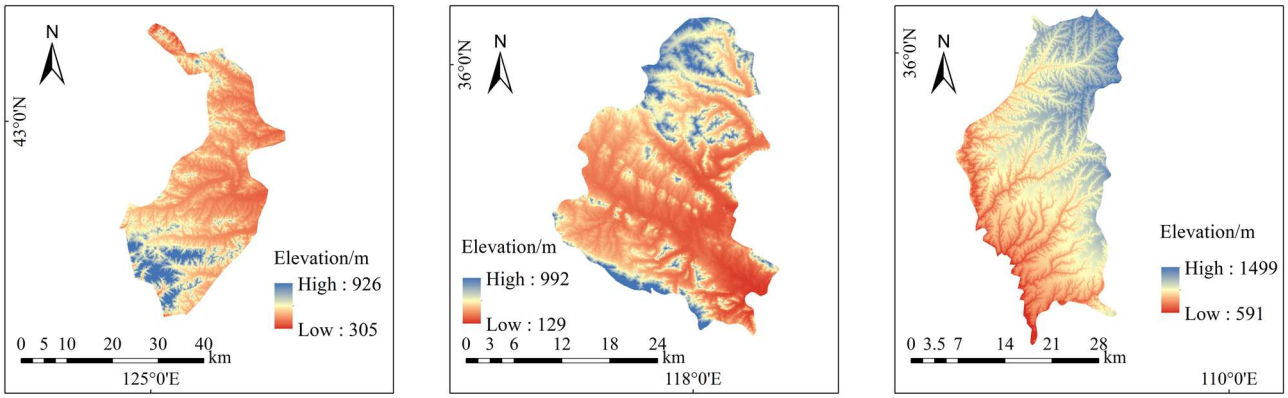

(**a**) (**b**) (**c**)

Figure 2. *Cont.*

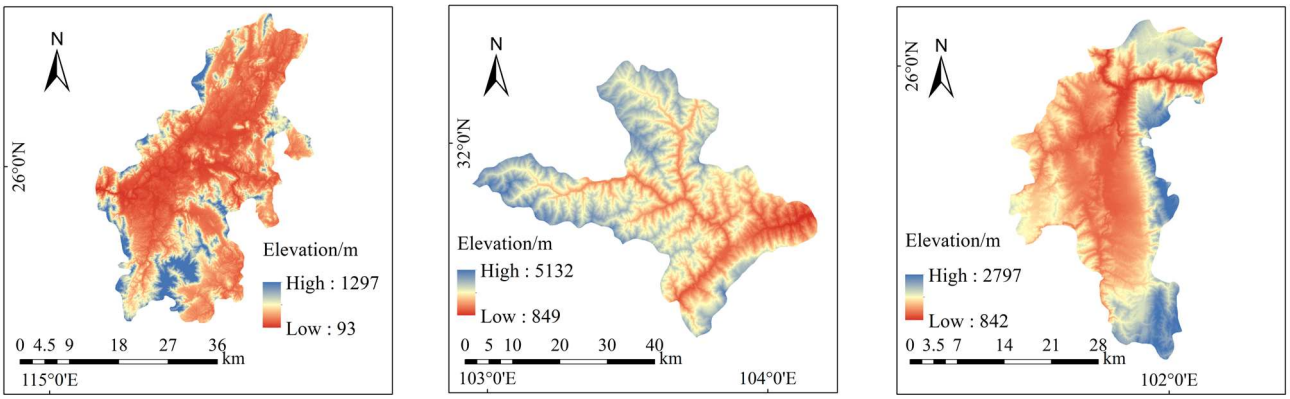

(**d**) (**e**) (**f**)

Figure 2. Maps of study sample areas showing location and altitude variation. (**a**) Dongfeng in NBSR; (**b**) Mengyin in NRMR; (**c**) Luochuan in NLPR; (**d**) Yudu in SRSR; (**e**) Maoxian in SPSR; (**f**) Yuanmou in SKMR.

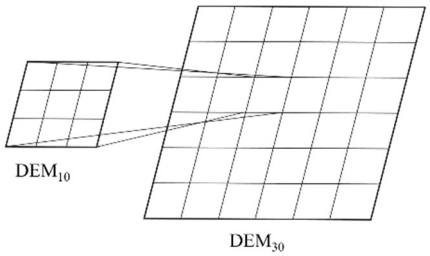

Figure 3. Raster correspondence between DEM_{30} and DEM_{10} (resampled by $DEM_{12.5}$).

The slope extracted by DEM should be classified before performing slope conversion and upscaling. According to the critical slope classification standard widely adopted in soil and water conservation in China, it can be divided into 9 grades: 0°–3°, 3°–5°, 5°–8°, 8°–15°, 15°–25°, 25°–35°, 35°–45°, 45°–60°, and >60°.

2.3. Third-Order Inverse Distance Square Weighted Difference Algorithm

Concerning the characteristics of DEM regular grid distribution, the third-order inverse distance square weighted difference algorithm (Figure 4) was used to extract slopes for DEM with different resolutions. Assuming that the coordinate of the central grid point (i, j) is (x_i, y_i), the local terrain surface expression is $z = f(x, y)$, and g is the grid spacing, then the primary Taylor series expansion at (i, j) is:

$$F(x_i + kg, y_i + kg) = f(x_i, y_i) + kgf_x + kgf_y \ (k = -1, 0, 1), \quad (1)$$

where f_x and f_y represent the partial derivatives of the topographic surface in x direction and y direction respectively; k represents the expansion range. Different mathematical models will be generated according to different values of k and weighting methods. The formula of the third-order inverse distance square weighted difference algorithm is as follows:

$$f_x = (z_{i-1,\,j+1} + 2z_{i,\,j+1} + z_{i+1,\,j+1} - z_{i-1,\,j-1} - 2z_{i,\,j-1} - z_{i+1,\,j-1})/8g, \quad (2)$$

$$f_y = (z_{i+1,\,j+1} + 2z_{i+1,\,j} + z_{i+1,\,j-1} - z_{i-1,\,j-1} - 2z_{i-1,\,j} - z_{i-1,\,j+1})/8g, \quad (3)$$

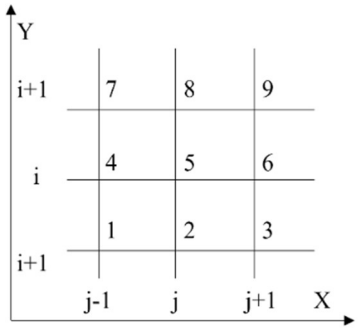

Figure 4. Schematic diagram of third-order inverse distance square weighted difference algorithm.

2.4. Mean and Standard Deviation Variation

The mean and standard deviation variation are defined as the variation of the mean and standard deviation of slopes caused by the change in unit resolution. The calculation formula is expressed as:

$$S_v = (S_{high} - S_{low})/(l - h) \quad (4)$$

where S_v represents the mean or standard deviation variation (°/m) and, the larger the value, the more drastic slope gradient changes with the resolution; S_h and S_l represent the slope gradient or standard deviation corresponding to high resolution and low resolution, respectively; l represents the cell size of low resolution, h represents the cell size of high resolution.

2.5. Slope-Conversion-Atlas

The concept of slope spectrum emerged due to the strong spatial autocorrelation of relief features in the same geomorphic type area [38], which can be combined through the slope quantity of different grades of the ground to reflect different slope proportion characteristics, and relief of the terrain in a certain region [53]. A "slope-conversion-atlas" is a map, chart, image or curve with conversion rules formed by combining graphic logic and information thinking based on geo-infographic maps, and arranged according to certain index grading or classification law. It can be used to represent the correlated conversion of slope under different spatial resolutions, different scale base maps and different geomorphological types [54,55]. The slope information extracted from different resolutions of DEM can be statistically analyzed through a "slope-conversion-atlas".

In this paper, the steps of "slope conversion mapping" are concretized by the formula. For each grade of slope with low resolution, the formula is as follows:

$$\begin{aligned} A_{hi} &= P_i A_{li} \\ \sum_{i=1}^{9} P_i &= 1 \end{aligned} \quad (5)$$

where A_{li} represents the area of each slope gradient grade with low resolution (90 m, 30 m); A_{hi} represents the corresponding area of the high resolution (10 m); P_i represents the frequency of conversion to 10 m resolution slope classes in each slope grade of low resolution; i represents slope gradient grading (9 slope grades).

The correction rate is calculated by the following formula:

$$C = \sum_{i=1}^{9} A_{li} * A_{hi}/A_{lx} * A_i \quad (6)$$

where C stands for the correction rate; Alx is the total area of each sample region in the low resolution; Ai represents the area of grids in the 10 m resolution slope class.

3. Results

3.1. Slope Scale Effect in Different Water Erosion Regions

3.1.1. Statistics of Slope Eigenvalues

Based on slope information extracted from three resolution DEM, maximum value, mean value, standard deviation, mean value, and standard deviation variation were selected as slope statistical characteristic values to express slope conditions in each water erosion regions. With the decrease in resolution, the maximum value, average value, and standard deviation of the overall slope in each sample region gradually decreased, except for the maximum value of the slope in SPSR, which was greater than that of $DEM_{12.5}$ at DEM_{30}. Among the six sample areas, due to the broken landform, the maximum slope amplitude of NLPR was the largest, and the slope decreased as much as 36.79° from $DEM_{12.5}$ to DEM_{90}. For the three resolutions, the maximum and minimum values of average slope gradient all appeared in SPSR and NBSR, respectively. Except for NBSR, the change in slope standard deviation from $DEM_{12.5}$ to DEM_{30} in each sample area was smaller than that from DEM_{30} to DEM_{90}, and the variation was most significant in NLPR (Table 1). Obviously, the topographic information gradually decreases with the reduction in resolution, and the slope shows attenuation phenomenon and gradual centralization.

Table 1. Statistical characteristic values of slope for different DEM resolutions.

Sample Region	Maximum Value (°)			Mean Value (°)			Standard Deviation			MCR (°/m)		SDV (°/m)	
	12.5 m	30 m	90 m	12.5 m	30 m	90 m	12.5 m	30 m	90 m	30 m	90 m	30 m	90 m
DF	50.76	45.87	27.29	6.61	5.26	4.45	5.89	4.67	4.16	0.077	0.014	0.070	0.009
MY	68.42	59.40	40.41	8.64	8.01	6.36	7.68	7.14	5.84	0.036	0.028	0.031	0.022
LC	72.15	61.38	35.36	15.33	15.11	10.99	10.35	9.05	6.81	0.013	0.069	0.074	0.037
YD	78.03	67.39	53.48	14.89	13.70	9.51	9.71	8.96	7.25	0.068	0.070	0.043	0.029
MX	85.46	87.05	70.87	32.39	31.49	29.67	12.38	12.11	9.88	0.051	0.030	0.015	0.037
YM	82.09	75.83	65.97	17.64	16.61	14.11	11.34	10.82	9.60	0.059	0.042	0.030	0.020

Notes: DF, MY, LC, YD, MX and YM in the table represent: Dongfeng, Mengyin, Luochuan, Yudu, Maoxian, and Yuanmou, and the other tables are expressed as this kind; MCV is mean change rate and SD is standard deviation variation.

For the six water erosion regions, the mean slope variation increased with the decrease in resolution in SRSR and NLPR, while it gradually decreased in other regions. The maximum mean variation from $DEM_{12.5}$ to DEM_{30} was found in NBSR (0.077) and the minimum in the NLPR (0.013). The standard deviation variation increases with the decrease in resolution in SPSR, which is contrary to other sample regions. The standard deviation variation both decreased from DEM_{30} to DEM_{90} by 0.009 in SKMR and NRSR, while it decreased by half in NLPR for the same transformation. It can be seen that with the decrease in slope resolution, the intensity of slope change also decreases, and the degree of decline is different in different regions, with the largest decline in NBSR and the least in NRSR.

The mean slope values obtained at different resolutions were regressed against the resolution to obtain the fitting formula between the mean slope and the resolution. The relationship between the average slope gradient and the resolution in each sample area was fitted (Table 2), and the results showed that the R2 of all regions was greater than 0.9, indicating a good fitting relationship. In general, with the decrease in resolution of DEM, the trend of average slope attenuation in each sample area was different. Among them, the average slope and resolution showed an exponential decline in SRSR and SKMR, and a linear decreasing relationship was found in the NRMR, SPSR and NLPR areas. In the NBSR, the relationship of logarithmic decline was observed.

Table 2. The fitting relationship between average slope and resolution in each study sample area.

Sample Area	Fitting Formula	R^2
DF	$y = -1.0791\ln(x) + 9.1911$	0.9566
MY	$y = -0.029x + 8.9503$	0.9973
LC	$y = -0.0592x + 16.426$	0.9704
YD	$y = 16.169e^{-0.006x}$	0.9977
MX	$y = -0.0339x + 32.687$	0.9866
YM	$y = 18.201e^{-0.003x}$	0.9975

Notes: In the table, x represents the average slope of each sample area at different resolutions; y denotes resolution.

3.1.2. Slope Frequency Curves and Cumulative Frequency Curves

Slope data of three spatial resolutions were used to generate the curve distribution diagram of frequency and cumulative frequency (Figure 5), which can intuitively reveal the variation rule of slope with resolution.

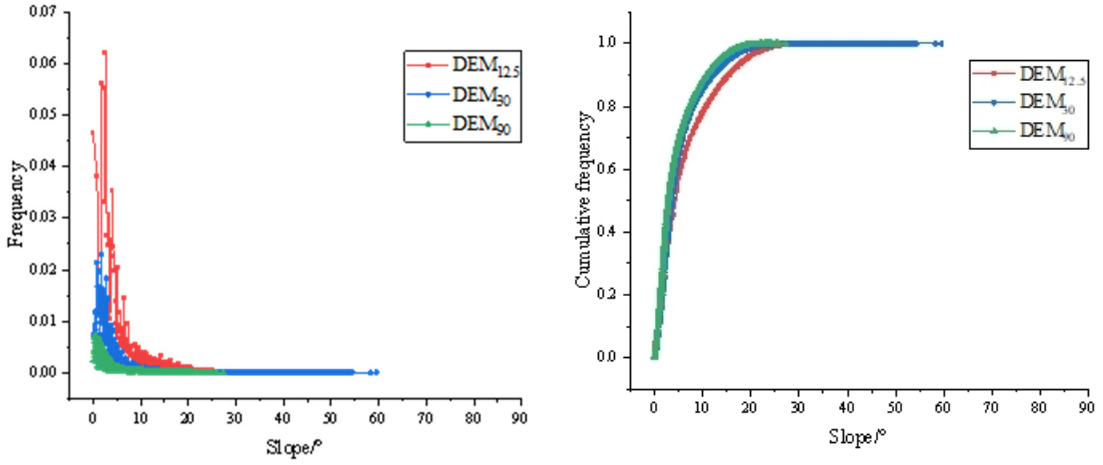

(**a**) Northeast Black Soil Region (Dongfeng)

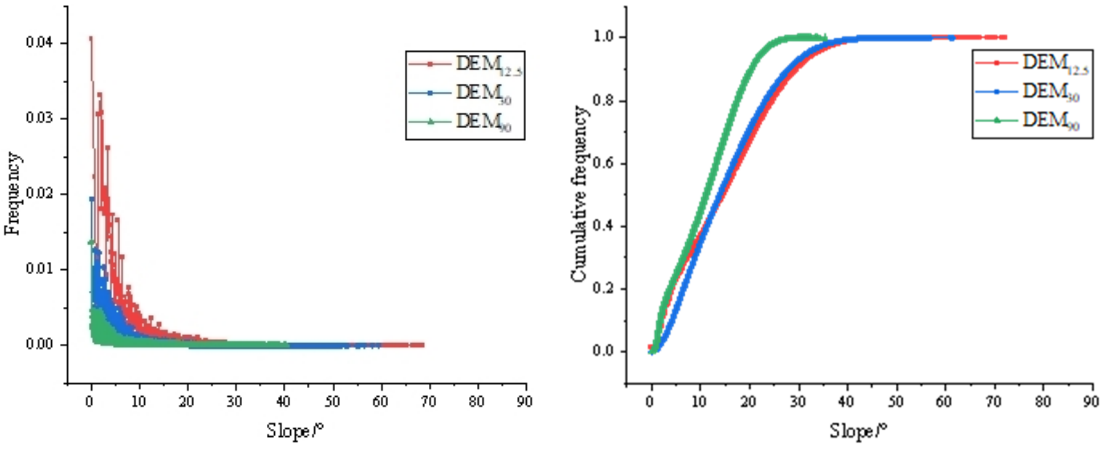

(**b**) North Rocky Mountain Region (Mengyin)

Figure 5. *Cont.*

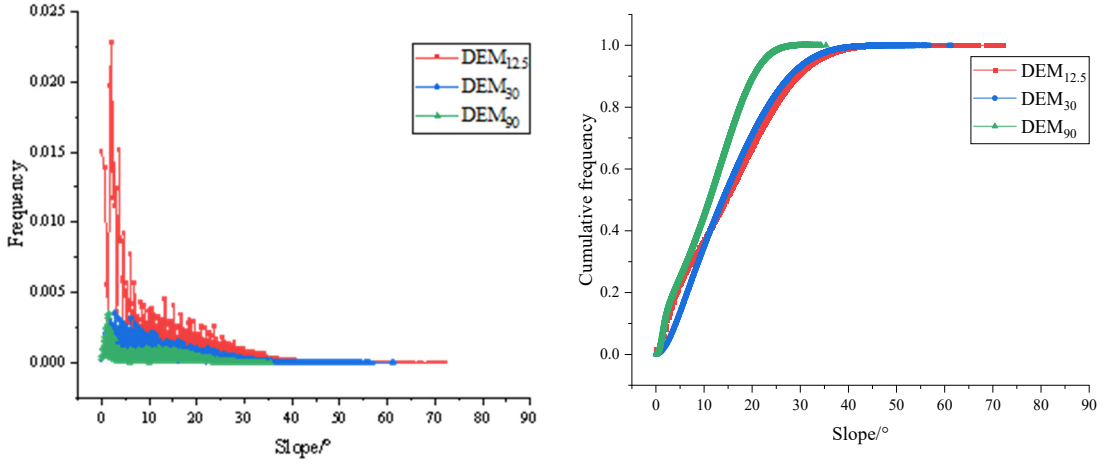

(**c**) Northwest Loess Plateau Region (Luochuan)

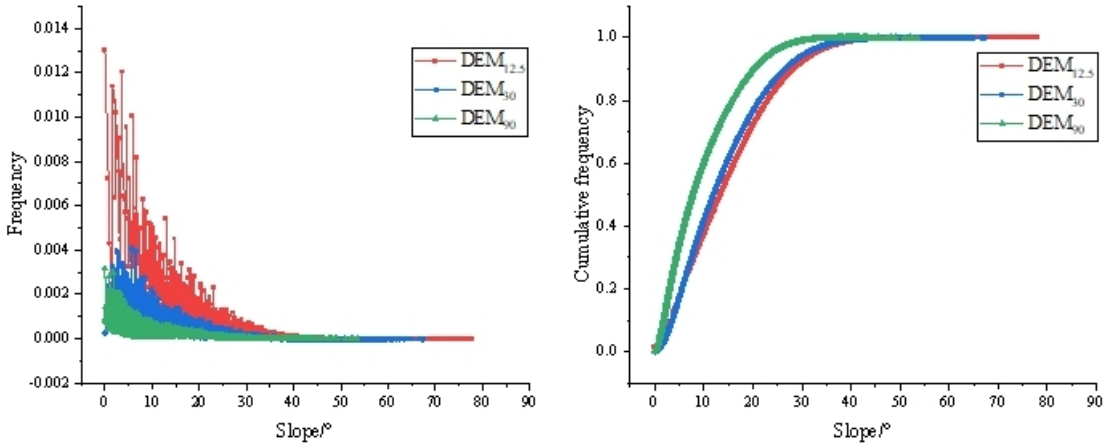

(**d**) Southern Red Soil Region (Yudu)

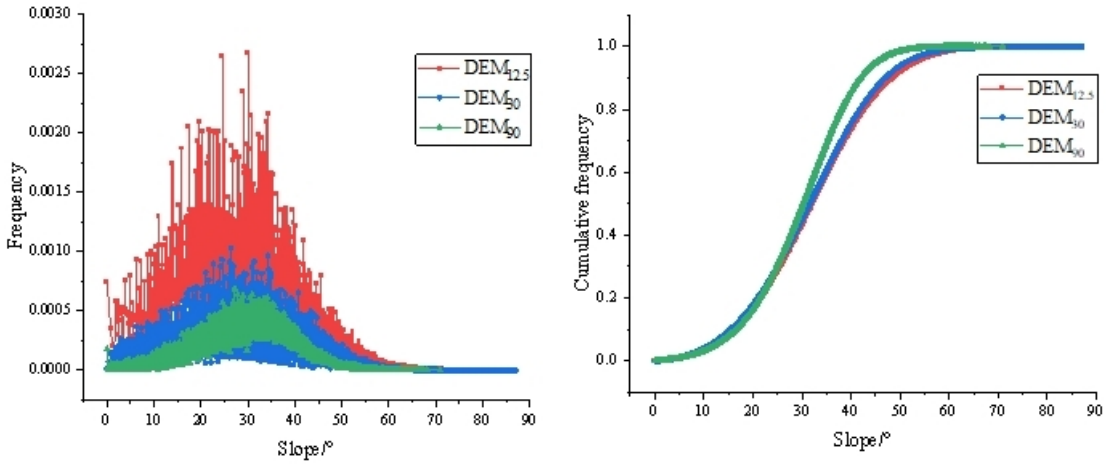

(**e**) Southwest Purple Soil Region (Maoxian)

Figure 5. *Cont.*

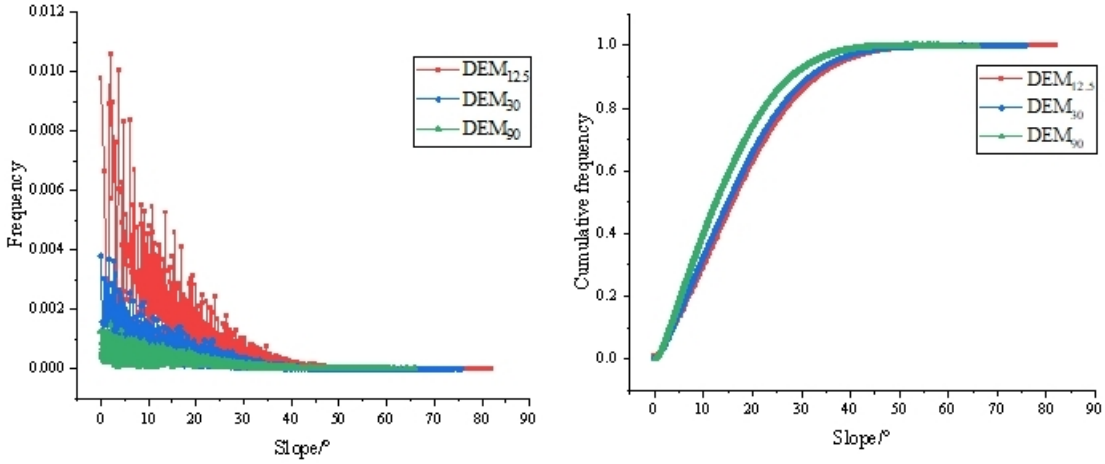

(**f**) Southwest Karst Mountainous Region (Yuanmou)

Figure 5. Slope frequency curves (**left**) and cumulative frequency curves (**right**) at different resolution for six water erosion regions.

As can be seen from the slope frequency curves, there are great differences in slope distribution among different sample areas. The peak value of frequency curve in both NBSR and NRMR are concentrated below 10°, and the maximum peak value of the $DEM_{12.5}$ frequency curve of NBSR is as high as 0.062. The peak value of frequency curve in NLPR, SKMR and SRSR are concentrated below 20°, which is similar to those of the former two regions, with a trend of gradually gentle with the increase in slope. The frequency curve in SPSR is similar to the normal distribution curve, mainly concentrated below 40°, and its maximum peak value is between 20° and 30°, which is significantly different from other sample areas. This may be related to the fact that the geomorphic types of the southwest purple soil areas are mainly high mountains and deep valleys. In general, with the decrease in the DEM resolution, the peak value of slope frequency curve in all areas are constantly moving towards the direction of small slope grades, and the peaks corresponding to slope frequency show an increasing trend, indicating that the distribution area of small slopes in all areas is also increasing.

What can be seen from the slope cumulative frequency curve is that the curve of DEM_{90} in all sample areas reaches the peak first, and the curve of $DEM_{12.5}$ reaches the peak last. With the decrease in resolution of DEM, the part with greater topographic changes gradually "disappear", making the topographic undulation tend to be gentle. The cumulative frequency curve all showed upward convexity in five regions, but in SPSR, it is convex first downward and then upward. The inflection point is about 25°, which almost coincides with the first peak of the frequency curve. At the same time, the three resolution curves show the distribution rules of slope grades under different DEM resolutions in each sample area. Among them, the cumulative frequency curves of $DEM_{12.5}$ and DEM_{30} in the northwest Loess Plateau region intersect at 10°~15°, and the slope distribution of $DEM_{12.5}$ is similar to that of DEM_{90} and DEM_{30}, respectively, on both sides of the intersection. In other sample regions, slope grade distribution in $DEM_{12.5}$ was similar to that in DEM_{30}.

3.2. Comparison of Slope-Conversion-Atlas for Different Regions

3.2.1. Conversion-Atlas Difference for Each Sample Area

To clarify the conversion of low-resolution slope grades to high-resolution slope grades, the slope conversion atlas was used for visual expression. In Figure 6, the horizontal axis represents the different slope grades for low resolution (DEM_{90}, DEM_{30}), while the legend on the right represents different slope grades of DEM_{10}. Each slope grade in each slope conversion map can be considered as a whole, and the vertical axis stands for the area percentage of each slope grade in the low resolution when converted to DEM10.

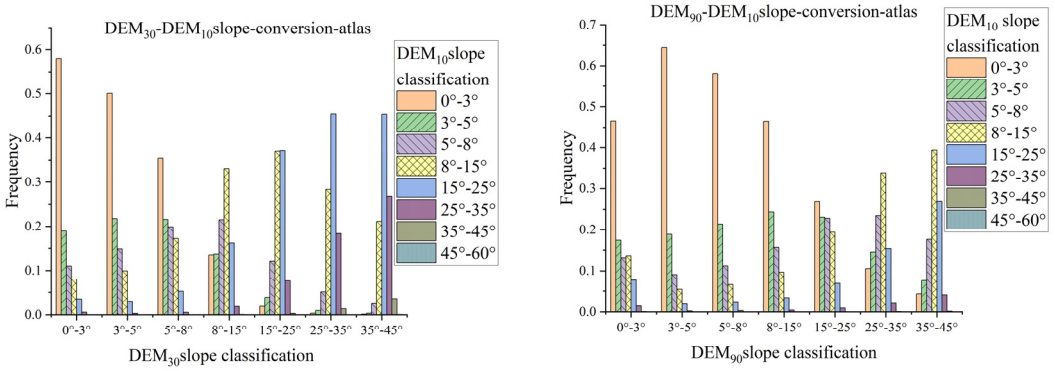

(**a**) Northeast Black Soil Region (Dongfeng)

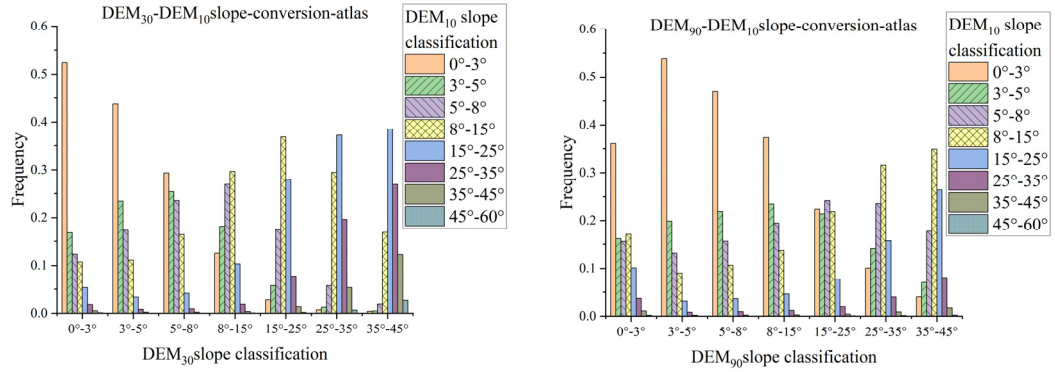

(**b**) North Rocky Mountain Region (Mengyin)

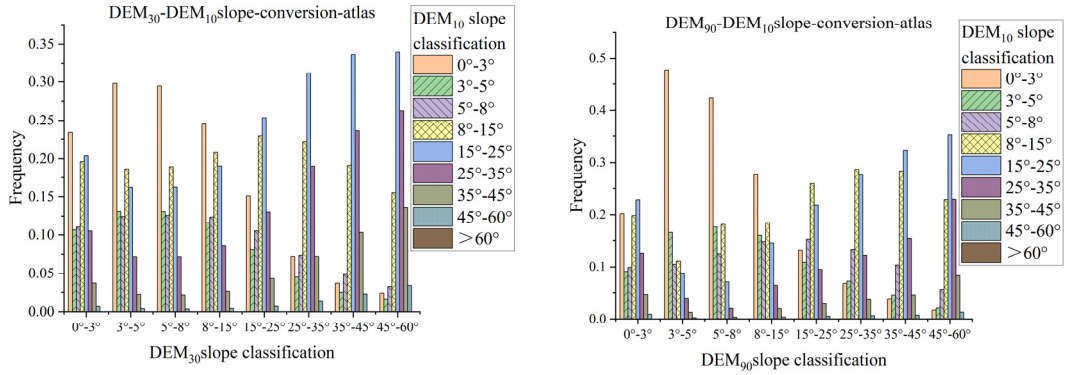

(**c**) Northwest Loess Plateau Region (Luochuan)

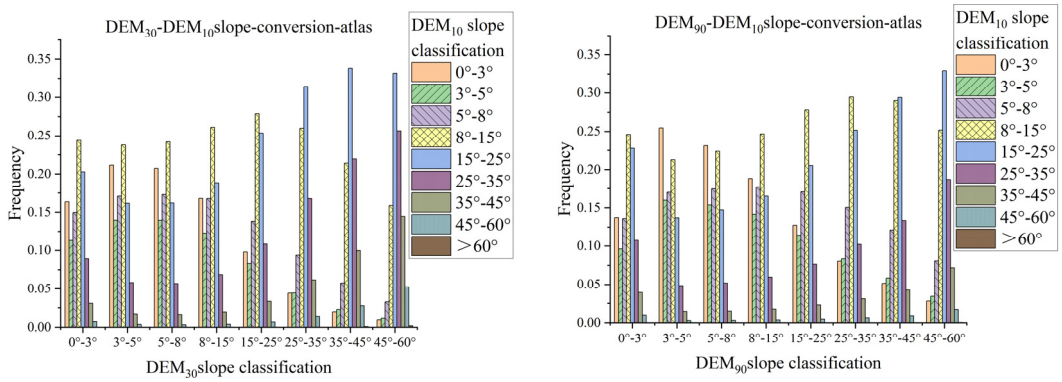

(**d**) Southern Red Soil Region (Yudu)

Figure 6. *Cont*.

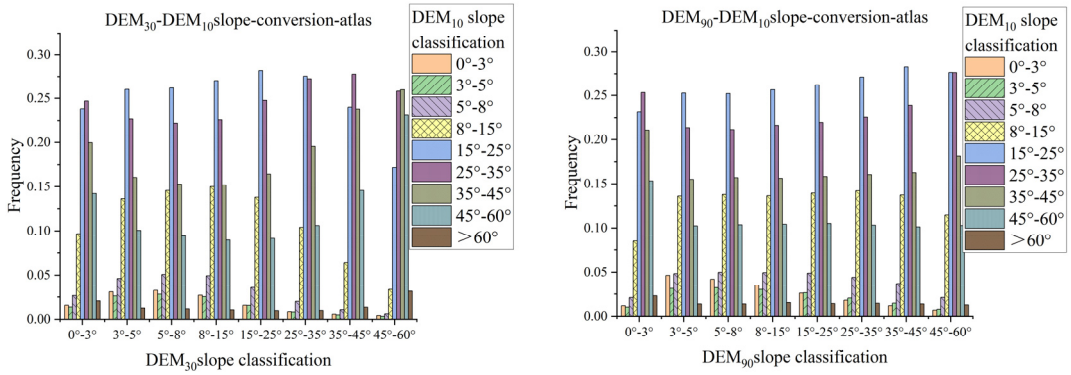

(**e**) Southwest Purple Soil Region (Maoxian)

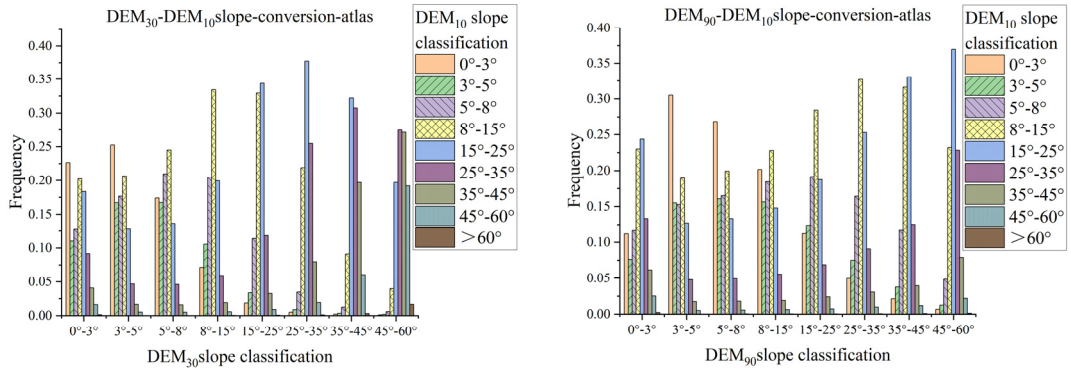

(**f**) Southwest Karst Mountainous Region (Yuanmou)

Figure 6. DEM_{30} to DEM_{10} (**left**) and DEM_{90} to DEM_{10} (**right**) slope-conversion-atlas for each sample region.

- NBSR and NRMR have similar distribution when DEM_{30} and DEM_{90} transition to DEM_{10}. The 0°–3° slope grade in DEM_{10} was mainly found at 0°–8° in DEM_{30} and 0°–25° in DEM_{90}. The highest frequency division occurs at 0°–3° in DEM_{30} and 3°–5° in DEM_{90}, respectively. In NLPR, the 15°–25° slope grade of DEM_{10} is mainly distributed in 15°–60° of DEM_{30}, while DEM_{90} is in 0°–3° and 35°–60°, which is related to the fact that the landform types are mainly loess beam hills and loess tableland, and the slope distribution is relatively discrete. For the conversion atlas of DEM_{30} and DEM_{90} of SPSR, the proportion of 15°–35° conversion to DEM_{10} of each slope grade is the largest (0.12~0.28). When upscaling DEM_{30} and DEM_{90} to DEM_{10} in SRMR, there are great differences in the slope composition of each grade. Only the 8°–15° slope grade transformed to DEM_{10} accounts for a larger proportion, with the maximum value up to 0.38. When upscaling to DEM_{10}, the 8°–15°grade occupies a relatively large proportion (0.16–0.29) in each grade of DEM_{30} and DEM_{90} in SRSR, mainly concentrated in the 0°–25° of DEM_{30}, 0°–3° and 15°–35° of DEM_{90}.
- Comparing the DEM_{30} to DEM_{10} slope conversion atlas of various regions, both similarities and differences can be found between them. The 0°–15° grade of DEM_{10} in NBSR, NLPR, NRMR, SKMR and SRSR mainly originated from the 0°–25° grade of DEM_{30}. Due to the geomorphic characteristics (a basin to the Tibetan Plateau climb), SPSR is different from other sample areas. The 0°–15° of DEM_{10} accounts for a small proportion (<0.15). By comparing the DEM_{90}-DEM_{10} slope conversion atlas of each sample area, a large difference also exists between SPSR and other sample areas. The 0°–8° and >60° of DEM_{10} occupy a very small proportion in each slope class of DEM_{90} (all <0.05). Meanwhile, NBSR, NLPR and NRMR share strong similarities; 0°–3° grade of DEM_{10} mainly transformed from 0°–25° of DEM_{90}, while SKMR is consistent with

SRSR, with 8°–15° of DEM_{10} accounting for a relatively large proportion in each slope grades of DEM_{90}.

- By analyzing the transformation atlas of each area, it is not difficult to find that the arrangement of slope grades has certain rules to follow. DEM_{30}-DEM_{10} is a conversion between adjacent resolutions, while DEM_{90}-DEM_{10} is a conversion across resolutions. However, the proportion of slope grades of low resolutions is larger when converting to lower slope grades (0°–25°) of DEM_{10}.

3.2.2. Slope Conversion Accuracy Analysis

In order to accurately reflect the distribution of the actual ground slope in each sample area, the slope obtained by DEM_{30} was graded according to the classification standards mentioned above, and the area of each slope grade of DEM_{30} or the percentage of the total area of the region can be obtained. Based on the DEM_{30}-DEM_{10} slope conversion atlas, each slope grade was converted, and the converted slope was summed up for each grade according to the slope grade of DEM_{10}, and eventually the distribution of slope in each slope grade in the region was obtained. The calculation steps were the same for the slope extracted by DEM_{90}.

The slope conversion atlas was used to correct the slope extracted with low resolution. The corrected results were firstly compared with each slope grade of DEM_{10}, and then the percentage of each slope grade in low resolution was taken as the coefficient, multiplied and then added with the previous ratio, to obtain the correction rate under the corresponding resolution (Table 3). As can be seen in Table 3, the average correction rate of DEM_{30} and DEM_{90} in all areas is above 90% and above 80%, respectively, indicating that the ground slope gradient retrieved from low resolution has been effectively corrected, and the correction effect of adjacent resolution is better.

Table 3. Correction effect of slope conversion atlas on the slope extracted by DEM_{30} and DEM_{90} (%).

Sample Area	DF		MY		LC		YD		MX		YM	
resolution	30 m	90 m	30 m	90 m	30 m	90 m	30 m	90 m	30 m	90 m	30 m	90 m
average correction rate	98.60	88.73	94.01	88.03	99.54	94.05	98.63	94.21	93.55	83.89	95.81	90.04

4. Discussion

Soil erosion, especially water erosion, is the main cause of land degradation and quantification of soil erosion rate plays a critical role in regional food security. Restricted by the heterogeneity and interaction of erosion factors, the data acquisition, availability, and quality in mountainous countries such as China have become the bottleneck of quantitative soil erosion research at a regional scale. Among them, topographic factors may be the most dominant factor affecting erosion for most cases in China. Although a wide variety of approaches have been employed to study regional scale erosion in different regions around the world, for a long time, quantitative erosion studies have been focused on the scales of plot size, hill-slope and catchment. At present, quantitative research on soil erosion at a regional scale mainly relies on empirical models such as USLE, RUSLE and CSLE, due to the data availability and their simplicity.

However, several problems arise when applying these models at a regional scale or larger scales. First, all model-based approaches imply uncertainties. Besides, considering the establishment conditions and applicable objects, especially empirical models only used to predict long-term annual soil loss on a single slope or plot. When applied to the study of regional scale erosion, slope parameters are generally extracted by low-resolution DEM. However, with the decrease in DEM resolution, the extracted slope decreases, which makes it unable to effectively reflect the actual relationship between topography and soil erosion, thus reducing the simulation accuracy of regional soil erosion.

In view of the above problems, this study combines digital image processing, digital terrain analysis, and geo-statistics theory. Through the systematic analysis of the rela-

tionship between slope and resolution, the slope attenuation law is understood, the slope attenuation mechanism is explained, and the slope distribution difference is analyzed. Combined with the histogram matching principle, the mathematical model of slope downscaling transformation is derived, making upscaling transformation of slope characteristics based on 90 m and 30 m similar statistical characteristics with 10 m resolution slope. The deficiency is that we did not compare generated slopes from different DEMs in a real erosion model due to data availability, since the study regions involve a nationwide area. In the future, we will continue to improve the collection of data on soil, precipitation, and erosion protection measures, as well as evaluate the practicability of slope upscaling transformation in a suitable model.

5. Conclusions

In this paper, on the basis of previous studies, we further studied the slope scale effect and slope conversion atlas for the six typical water erosion regions in China. The study area is large and widely distributed, which is unprecedented. We first extracted slope information based on DEM data of three resolutions, and slope scale issue was studied by analyzing slope changes with spatial resolution, as well as the differences and commonalities in conversion atlas for different erosion regions. The slope extracted with coarse resolution was then corrected by a grading method, so that the slope can reflect the terrain more accurately after correction and help to the regional scale erosion assessment. Lastly, differences and uncertainties for real soil erosion assessing situation were discussed. The main findings are summarized as follows:

(1) The slope scaling effect in various areas shows that with the decrease in resolution, the mean value and standard deviation of slope decrease, and the intensity of the change also decreases, and slope attenuation occurs. This is consistent with the results in previous studies [56,57]. The fitting results of average slope and resolution show that the slope attenuation speed is different in different areas, but the fitting effect is sound in all areas, with a R^2 greater than 0.9. According to the slope frequency curve and cumulative frequency curve, the proportion of low slope grades increases with the decrease in resolution, steep slope grades gradually decreases, and the topographic relief tends to be gentle.

(2) The similarity and difference of slope conversion atlas in different sample areas coexist under the same resolution. Except for SPSR, the similarity between different sample areas is relatively large, which is closely related to the resolution and the landform type, and is consistent with the experiments from local experts [23,29]. During the process of conversion, the proportion of conversion from DEM30 and DEM90 to the middle and low grades of DEM10 (0°–25°) is large. The grading correction based on the transformation atlas makes the correction precision of all areas more than 80% under different resolutions, and the correction effect of adjacent resolutions is better.

(3) On the basis of analyzing and understanding the scaling effect of slope and its variation with resolution, the slope transformation map method is used to obtain better grading correction results, which is of great significance for improving the accuracy of slope data in complex topographic areas and effectively formulating regional resource and environment planning. At present, this method does not have a good mathematical model to express the final corrected results, so the results cannot be inverted to spatial model, which will be a direction of further research.

Author Contributions: G.C. designed the entire framework and contributed significantly to the data collection; X.C. conducted experiments and wrote the manuscript; G.C. and J.F. has given many valuable suggestions for improving and modifying this paper. J.Z. and Y.W. contributed extensively to data processing. All the authors were involved in result analysis and discussion. All authors have read and agreed to the published version of the manuscript.

Funding: This research was supported by the Basic Research Project of Yunnan Province (Grant No. 202101AU070161) and the Strategic Priority Research Program of Chinese Academy of Sciences (Grant No. XDA26050301-01).

Data Availability Statement: All data used in this study are detailed in the manuscript.

Acknowledgments: We acknowledge the platform provided by Faculty of Land Resource Engineering of Kunming University of Science and Technology. We also want to thank the reviewers for their insightful contributions and suggestions.

Conflicts of Interest: The authors declare no conflict of interest.

References

1. Cao, Z.H.; Zhao, X.; Ding, S.Y.; Zhang, Y.F. The relative contributions of slope gradient and vegetation cover on erosion characteristics of riparian slopes along the lower Yellow River, China. 2021. Available online: https://www.authorea.com/doi/full/10.22541/au.162126546.69002458 (accessed on 1 June 2022).
2. Albut, S. Estimation of Slope Length (L) and Slope Steepness Factor (S) of RUSLE Equation by QGIS. *Int. J. Eng. Res. Gen. Sci.* **2020**, *8*, 43–48.
3. Luo, W.Q.; Jiang, Z.C.; Yang, Q.Y.; Li, Y.Q. The features of soil erosion and soil leakage in karst peak-cluster areas of Southwest China. *J. Groundw. Sci. Eng.* **2018**, *6*, 18–30.
4. Li, A.; Zhang, X.C.; Liu, B.Y. Effects of DEM resolutions on soil erosion prediction using Chinese Soil Loss Equation. *Geomorphology* **2021**, *384*, 107706. [CrossRef]
5. Wang, Z.H.; Luo, D.; Xiong, K.N.; Gu, X.; Zhu, Z.Z. Studies on Hydrological Processes on Karst Slopes for Control of Soil and Water Loss. *Sustainability* **2022**, *14*, 5789. [CrossRef]
6. Raj, A.R.; George, J.; Raghavendra, S.; Kumar, S. Effect of dem resolution on LS factor computation. *Int. Arch. Photogramm. Remote Sens. Spat. Inf. Sci.* **2018**, *42*, 315–321. [CrossRef]
7. Li, W.; Wang, R.L.; Liang, M.Z.; Niu, D.Q.; He, X.Y.; Ji, Z.; Luo, Z.M. Application of Topographic Factors in Soil and Water Loss Evaluation of Lushan County. *Anhui Agri. Sci. Bull.* **2021**, *16*, 168–171.
8. Yap, L.; Kande, L.H.; Nouayou, R.; Kamguia, J.; Ngouh, N.A.; Makuate, M.B.J. Vertical accuracy evaluation of freely available latest high-resolution (30 m) global digital elevation models over Cameroon (Central Africa) with GPS/leveling ground control points. *Int. J. Digit. Earth* **2019**, *12*, 500–524. [CrossRef]
9. Grohmann, C.H. Effects of spatial resolution on slope and aspect derivation for regional-scale analysis. *Comput. Geosci.* **2015**, *77*, 111–117. [CrossRef]
10. Buakhao, W.; Kangrang, A. DEM Resolution Impact on the Estimation of the Physical Characteristics of Watersheds by Using SWAT. *Adv. Civ. Eng.* **2016**, *2016*, 1–9. [CrossRef]
11. Yang, Q.K.; Guo, M.H.; Li, Z.G.; Wang, C.M. Extraction and preliminary analysis of topographic factors of soil erosion in China. *Soil Water Conserv. China* **2013**, *10*, 17–21.
12. Shan, L.X.; Yang, X.H.; Zhu, Q.G.Z. Effects of DEM resolutions on LS and hillslope erosion estimation in a burnt landscape. *Soil Res.* **2019**, *57*, 797–804. [CrossRef]
13. Xiong, K.N.; Li, J.; Long, M.Z. Features of Soil and Water Loss and Key Issues in Demonstration Areas for Combating Karst Rocky Desertification. *Acta Geogr. Sin* **2012**, *7*, 878–888.
14. Chang, K.T.; Merghadi, A.; Yunus, A.P.; Pham, B.T.; Dou, J. Evaluating scale effects of topographic variables in landslide susceptibility models using GIS-based machine learning techniques. *Sci. Rep.* **2019**, *9*, 12296. [CrossRef]
15. Liu, X.J.; Lu, H.X.; Ren, Z.; Ren, Z.F. Scale issues in digital terrain analysis and terrain modeling. *Geogr. Res.-Aust.* **2007**, *3*, 433–442.
16. Guo, Z.; Adhikari, K.; Chellasamy, M.; Greve, M.B.; Owens, P.R.; Greve, M.H.J.G. Selection of terrain attributes and its scale dependency on soil organic carbon prediction. *Geodrma* **2019**, *340*, 303–312. [CrossRef]
17. Drover, D.R.; Jackson, C.R.; Bitew, M.; Du, E. Effects of DEM scale on the spatial distribution of the TOPMODEL topographic wetness index and its correlations to watershed characteristics. *Hydrol. Earth Syst. Sci. Discuss.* **2015**, *12*, 11817–11846.
18. Nazari-Sharabian, M.; Taheriyoun, M.; Karakouzian, M. Sensitivity analysis of the DEM resolution and effective parameters of runoff yield in the SWAT model: A case study. *J. Water Supply* **2020**, *69*, 39–54. [CrossRef]
19. UCGIS. Research priorities for geographic information science. *Cartogr. Geogr. Inf. Syst.* **1993**, *23*, 115–127.
20. Zhang, J.X.; Chang, K.T.; Wu, J.Q. Effects of DEM resolution and source on soil erosion modelling: A case study using the WEPP model. *Int. Geogr. Inf. Sci.* **2008**, *22*, 925–942. [CrossRef]
21. Shi, X.; Girod, L.; Long, R.; DeKett, R.; Philippe, J.; Burke, T. A comparison of LiDAR-based DEMs and USGS-sourced DEMs in terrain analysis for knowledge-based digital soil mapping. *Geoderma* **2012**, *170*, 217–226. [CrossRef]
22. Qinke, Y.; Jupp, D.; Rui, L.I.; Wei, L. Re-scaling lower resolution slope by histogram matching. In *Advances in Digital Terrain Analysis*; Springer: Berlin/Heidelberg, Germany, 2008; pp. 193–210.
23. Wolock, D.M.; McCabe, G.J. Differences in topographic characteristics computed from 100- and 1000-m resolution digital elevation model data. *Hydrol. Process.* **2000**, *14*, 987–1002. [CrossRef]

24. Mukherjee, S.; Mukherjee, S.; Garg, R.D.; Bhardwaj, A.; Raju, P.L.N. Evaluation of topographic index in relation to terrain roughness and DEM grid spacing. *J. Earth Syst. Sci.* **2013**, *122*, 869–886. [CrossRef]
25. Zhang, X.X.; Song, J.X.; Wang, Y.R.; Deng, W.J.; Liu, Y.F. Effects of land use on slope runoff and soil loss in the Loess Plateau of China: A meta-analysis. *Sci. Total Environ.* **2020**, *755*, 142418. [CrossRef]
26. Fu, S.H.; Cao, L.X.; Liu, B.Y.; Wu, Z.P.; Savabi, M.R. Effects of DEM grid size on predicting soil loss from small watersheds in China. *Environ. Earth Sci.* **2014**, *73*, 2141–2151. [CrossRef]
27. Tang, G.A.; Zhao, M.D.; Li, T.W.; Liu, Y.M.; Xie, Y.L. Modeling Slope Uncertainty Derived from DEMs in Loess Plateau. *Acta Geogr. Sin.* **2003**, *6*, 824–830.
28. Wu, W.; Fan, Y.; Wang, Z.Y.; Liu, H.B. Assessing effects of digital elevation model resolutions on soil–landscape correlations in a hilly area. *Agric. Ecosyst. Environ.* **2008**, *126*, 209–216. [CrossRef]
29. Quinn, P.; Beven, K.; Chevallier, P.; Planchon, O. The prediction of hillslope flow paths for distributed hydrological modelling using digital terrain models. *Hydrol. Process.* **1991**, *5*, 59–79. [CrossRef]
30. Lu, S.J.; Liu, B.Y.; Hu, Y.X.; Fu, S.H.; Cao, Q.; Shi, Y.D.; Huang, T.T. Soil erosion topographic factor (LS): Accuracy calculated from different data sources. *Catena* **2020**, *187*, 104334. [CrossRef]
31. Wu, J.; Fang, J.J.; Tian, J.B. Terrain Representation and Distinguishing Ability of Roughness Algorithms Based on DEM with Different Resolutions. *AGR Ecosyst. Environ.* **2019**, *8*, 180. [CrossRef]
32. Yin, Z.Y.; Wang, X. A cross-scale comparison of drainage basin characteristics derived from digital elevation models. *Earth Surf. Process. Landf.* **2015**, *24*, 557–562. [CrossRef]
33. Longley, P.A.; Goodchild, M.F.; Maguire, D.J.; Rhind, D.W. *Geographic Information Science and Systems*; John Wiley & Sons: Hoboken, NJ, USA, 2015.
34. Zhang, Y. A Research Slope Spectrum of the Loess Plateau. Master's Thesis, Northwestern University, Xi'an, China, 2003.
35. Guo, L.Q.; Yang, Q.K.; Hu, J.; Lan, M.; Liu, H.Y.; Li, J. Research on method of re-scaling coarser resolution slope based on fractal analysis approach. *J. Northwest Sci.-Tech. Univ. Agric. For.* **2011**, *12*, 173–180.
36. Zhang, X.Y.; Drake, N.A.; Wainwright, J.; Mulligan, M. Comparison of slope estimates from low resolution DEMs: Scaling issues and a fractal method for their solution. *Earth Surf. Proc. Land.* **1999**, *24*, 763–779. [CrossRef]
37. Klinkenberg, B.; Goodchild, M.F. The fractal properties of topography: A comparison of methods. *Earth Surf. Process. Landf.* **2010**, *17*, 217–234. [CrossRef]
38. Tang, G.A.; Li, F.Y.; Liu, X.J.; Long, Y.; Yang, X. Research on the slope spectrum of the Loess Plateau. *Sci. China Ser. E* **2008**, *51*, 175–185. [CrossRef]
39. Tang, G.A.; Yang, Q.K.; Zhang, Y.; Liu, Y.M.; Liu, X.H. Research on Accuracy of Slope Derived From DEMs of Different Map Scales. *Bull. Soil Water Conserv.* **2001**, *1*, 53–56.
40. Chen, Y.; Qi, Q.W.; Tang, G.A. Research on slope-conversion-atlas in Loess Plateau. *Agric. Res. Arid Areas* **2004**, *3*, 180–185.
41. Meng, T.T.; Jin, M.H.; Cheng, J. Fractal characteristics of soil particle size in loess hilly areas with different years of conversion. *IOP Conf. Ser. Earth Environ. Sci.* **2021**, *692*, 042070. [CrossRef]
42. Wang, C.M. Slope Scaling Effect, Transformation and the Influence to Soil Erosion Assessment. Ph.D. Thesis, Graduate School of Chinese Academy of Sciences (Center for Soil and Water Conservation and Ecological Environment Research, Ministry of Education), Xianyang, China, 2012.
43. Hu, Y.H.; He, X.B.; Bi, J.Z. Assessment on the Accuracy of the Histogram Matching Algorithm for slope Correction. *Res. Soil Water Conserv.* **2013**, *6*, 97–101.
44. Liu, F.; Fan, J.R.; Cui, Z.Y.; Cheng, D.X.; Tang, J.Y. A Model of Re-Scaling Slope Based on DEM Fractal Feature. *J. Mount. Sci.* **2019**, *1*, 129–136.
45. Roostaee, M.; Deng, Z.Q. Effects of digital elevation model resolution on watershed-based hydrologic simulation. *Water Resour. Manag.* **2020**, *34*, 2433–2447. [CrossRef]
46. Liu, A.L.; Tang, G.A.; Qin, H.R. Research on Scaling of Digital Slope Conversion Models under Different Grid Resolution. *J. Soil Water Conserv.* **2002**, *16*, 4.
47. Liu, X.H. Analysis and Extraction of Topographic in Regional Soil and Water Loss. Master's Thesis, Northwest Agriculture and Forestry University of Science and Technology, Xianyang, China, 2001.
48. Niu, S.M.; Zhong, W.Z.; Liu, Q.L.; Zhao, X.Y. Research on Correction of Slope Statistics Error Based on Conversion Arithm etic. *Geod Vestn.* **2008**, *7*, 29–31.
49. Shi, W.J. The Study on Slope Rescaling Based on DEM and GIS Methods. Master's Thesis, Northwest Agriculture and Forestry University of Science and Technology, Xianyang, China, 2007.
50. Panuska, J.C.; Moore, I.D.; Kramer, L.A. Terrain analysis: Integration into the agricultural nonpoint source (AGNPS) pollution model. *J. Soil Water Conserv.* **1991**, *46*, 59–64.
51. Yang, L.H. LS factor Scale Transformation and Application in Soil Erosion Sampling Survey. Master's Thesis, University of Chinese Academy of Sciences (Research Center for Soil and Water Conservation and Ecological Environment, Ministry of Education, Chinese Academy of Sciences), Xianyang, China, 2020.
52. Zhao, Y.J.; Cong, P.J.; Feng, W.; Chang, D.D.; Wang, H.Y. Identification and distribution of counties with severe soil erosion. *Soil Water Conser. China* **2018**, *3*, 20–24.
53. Tang, G.A.; Li, F.Y.; Xiong, L.Y. Progress of Digital Terrain Analysis in the Loess Plateau of China. *Geogr. Geo-Inf. Sci.* **2017**, *4*, 1–7.

54. Chen, S.P.; Yue, T.X.; Li, H.G. Studies on Geo-Information Tupu and its application. *Geogr. Res.-Aust.* **2000**, *4*, 337–343.
55. Qi, Q.W.; Chi, T.H. Research on the Theory and method of Geo-Info-TUPU. *Acta Geogr. Sin* **2001**, *56*, 8–18.
56. Yang, C.J.; Zhao, X.L.; Zhou, Q.L.; Ni, J. Analysis of Scale Effect Charateristics of DEM and Slope in Hilly Areas. *J. Geo-Inf. Sci.* **2013**, *15*, 814–818.
57. Wang, S.; Zhu, X.; Zhang, W.; Yu, B.; Fu, S.; Liu, L. Effect of different topographic data sources on soil loss estimation for a mountainous watershed in Northern China. *Environ. Earth Sci.* **2016**, *75*, 1–12. [CrossRef]